Computational modeling of passive furrowed channel micromixers for lab-on-a-chip applications

Francesca Nason, Giancarlo Pennati, Gabriele Dubini

Laboratory of Biological Structure Mechanics, Department of Chemistry, Materials and Chemical Engineering Giulio Natta, Politecnico di Milano, Milano - Italy

INTRODUCTION

The recent trend in analytical chemistry and life sci-ence has been toward miniaturization of fluid handling and analysis, which has emerged in the field of microfluid-ics. Microfluidic applications cover micro arrays, sample preparation and analysis, cell separation and detection, and environmental monitoring (1). Most microfluidic systems operate in a laminar flow regime dominated by molecular diffusion, which is not favorable to mixing (2). Mixing is a key process for the success of all chemical or biochemical reactions. The absence of turbulence, the pri-mary mechanism for macroscale mixing, has spurred re-searchers to investigate alternative strategies for mixing in microfluidic systems. Hence, effective micromixers represent essential components for micro total analysis systems or lab-on-a-chip.

Recently, our group developed a microfluidic platform for drug screening to perform pharmacological in vitro tests on cells (3). The device, conceived to identify the concentration range in which the drug effectiveness is guaranteed, allows the simultaneous testing of multiple concentrations: namely, 5 different drug concentrations were considered, and 45 wells were adopted, to perform both viability tests and proliferation tests on cell cultures. To get the desired concentration levels, different medium and drug flows are spilled from the 2 main fluid lines and join in a channel which reaches the wells. Due to the choices concerning the geometry of the device, little space is available on the platform; therefore it is necessary to provide an efficient mixing system to assure an homogeneous flow to the cells.

In general, micromixers can be classified as active or passive. The former use an external source to generate

Accepted: March 7, 2013

Address for correspondence:
Giancarlo Pennati
Laboratory of Biological Structure Mechanics
Department of Chemistry, Materials and
Chemical Engineering “Giulio Natta”
Politecnico di Milano
Piazza Leonardo da Vinci, 32
IT-20133 Milano, Italy
giancarlo.pennati@polimi.it

a disturbance on the fluid field to enhance the mixing process, while the latter rely entirely on diffusion or chaotic advection (4, 5), and achieve mixing by exploiting only the geometry of the channel (1). In particular, passive micromixers aim to increase the interface between the 2 fluids that have to be mixed so as to improve molecular diffusion and reduce the mixing length of channel required. Examples of such micromixers are serial or parallel laminating (6), split and recombine (7) and chaotic, recirculation flow mixers (8). Passive mixers are used in most microfluidic applications, since they can be easily produced, cleaned and integrated into microfluidic systems (9). Both numerical and experimental approaches can be found in the literature to investigate micromixer performances and to optimize their design. As an example, Liu et al studied numerically and experimentally the mixing process in a 3-dimensional serpentine microchannel design (10). In particular, a C-shaped repeating unit was adopted as a means of implementing chaotic advection to passively enhance fluid mixing. Generally, the mixing capability of a channel increases with increasing Reynolds number: the presence of secondary flows is essential to obtain a fast and efficient mixing in microchannels (11). Some recent studies (9, 12) have focused on the parametrical study of particular geometries to increasingly amplify the stirring ability of a mixer.

In the present work, numerical analyses of mixing in a 3-dimensional channel with obstacles on the walls were performed to investigate mixing behavior and flow characteristics with geometric parameters as well as Reynolds number.

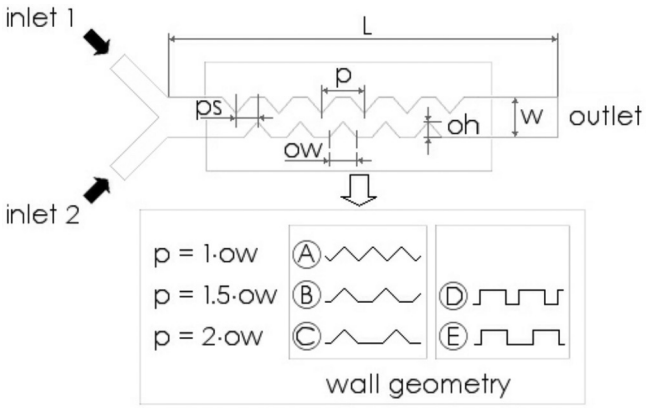

Fig. 1 - *Sketch of the geometries considered. L = length; p = pitch; ps = phase shift; ow = obstacle width; oh = obstacle height; w = width.*

TABLE I - SUMMARY OF THE PARAMETER VALUES ADOPTED IN THE NUMERICAL SIMULATIONS

Pitch	*p/ow*	1	1.5	2
Phase shift	*ps*	0°	90°	180°
Obstacle dimension	*oh/w*	0.2	0.3	0.4
Aspect ratio	*h/w*	1/3	2/3	1
Reynolds number	Re	10	50	100

p = pitch; ow = obstacle width; ps = phase shift; oh = obstacle height; w = width; h = height.

MATERIAL AND METHODS

Micromixer geometries

A number of micromixers were modeled consisting of 2 inlets converging in a furrowed channel (Fig. 1) with fixed whole dimensions: width *w* and length *L* equal to 150 μm and 3.2 mm, respectively. The walls of the channel were furrowed due to the presence of obstacles. Five different wall geometries were investigated (from A to E) with triangular or rectangular obstacles. In particular, triangular and rectangular obstacles presented a fixed width to height ratio, namely *ow*/*oh* = 3/5. The geometries considered correspond to different values for the pitch *p* of the furrowed wall, expressed as *p*/*ow* equal to 1, 1.5 and 2. Evidently, the configuration with *p*/*ow* equal to 1 cannot be defined for the rectangular obstacles, leading to a smooth wall.

Moreover, different channel configurations were considered according to different values for wall phase shift and aspect ratio (Tab. I).

The adopted parametric modeling approach allowed a systematic investigation of a large number of micromixer geometries. However, since the number of possible configurations is huge, a number of consecutive sets of simulations were performed to limit the parameter range and identify the best configurations to use in additional analyses. The first computational analyses were performed to investigate the influence of the phase shift between the 2 facing walls (*ps* equal to 0°, 90° and 180°) for the 5 wall geometries (keeping fixed *h*/*w* and *oh*/*w* at 1/3 and 0.4, respectively) and 2 Reynolds numbers (Re equal to 10 and 50). Subsequently, the effects of the obstacle dimension *oh* and channel height *h* were considered. Namely, 3 obstacle dimensions *oh* (20%, 30% and 40% of the channel width) and 3 different heights of the channels *h* (50, 100 and 150 μm, corresponding to different aspect ratios *h*/*w*) were investigated.

These simulation sets allowed us to point out the best *ps*, *oh*/*w* and *h*/*w* values for which an enhanced mixing occurs. Afterwards, for the 2 channel configurations showing the best performances, a number of additional analyses were performed to compare mixing performances.

NUMERICAL METHODS

Simulation parameters

Computer-aided design (CAD) models of each configuration and their meshes were generated by means of the solid modeler GAMBIT (Ansys Inc., Canonsburg, PA, USA). Domains were discretized using a structured mesh of hexahedral elements. The stability of the fluid flow solution on a structured mesh is essentially higher than that on an unstructured mesh; moreover, a structured mesh allows one to better control the spatial arrangement of the elements (12).

The numerical simulations of the flow and advection-diffusion process in the micromixers were performed using ANSYS Fluent 12.1 (ANSYS, 2010). This is a general purpose commercial computational fluid dynamics (CFD) modeling package which allows the solution of Navier-Stokes equations using a finite volume method via a coupled solver. Steady-state momentum and continuity equations for the fluid flow in the micromixers were solved. Subsequently, the diffusion-advection equation was solved with an uncoupled approach. The advection terms in each equation were discretized using an up-wind scheme with a second order correction to minimize numerical errors (13). Simulations were typically considered to have attained convergence as the normalized residuals for velocities and species fell below 1×10^{-7}. The analyses were run on a Linux cluster (1 node with 2 Quad-Core Intel Xeon processors, 8 GB RAM).

A uniform velocity profile normal to the cross-sections was imposed at both inlets. No-slip boundary conditions were applied at all walls, while a uniform pressure condition (P=0) was imposed at the outlet of the channel.

The 2 working fluids are deionized water and a dye dissolved in water. Regarding the advection diffusion, a single-phase model was adopted: the boundary conditions for the species balance are mass fractions equal to 0 at the inlet where pure water is fed and equal to 1 at the inlet where the dye is fed. The diffusion coefficient was set to $D = 1.5\times10^{-9}$ m²/s.

A preliminary grid convergence study was carried out to verify that the solution was grid independent. In fact, highly refined meshes were needed to get accurate results, especially for advection-diffusion analyses. In particular, the change in the mixing quality values was found to be less than 0.001 when increasing by 10% the number of cells. Therefore, a grid with almost 4×10^{6} elements was obtained (the size of the element was approximately 1.67×1.67 μm).

Evaluation of micromixer performances

To evaluate the homogeneity of the mixing patterns, the spread of the dye was quantified calculating the variance in a cross-section of the mixing channel perpendicular to the main flow. This is based on the concept of the intensity of segregation, which is related to the variance of the concentration with respect to the mean concentration. To evaluate the degree of mixing in the micromixer, the variance of the mass fraction of the mixture in a cross-section normal to the flow direction was defined as:

$$\sigma = \sqrt{\frac{1}{N}\sum (c_i - \bar{c}_m)^2}, \qquad [1]$$

where N is the number of sampling points inside the cross-section, c_i is the mass fraction at sampling point i and $\bar{c}_m$ is the optimal mixing mass fraction.

In this work, N was 1,350, 2,700 and 4,050 for h equal to 50, 100 and 150 μm, respectively, so that high accuracy was ensured. The sampling points were taken equidistant on the cross-sectional plane, and the values at the sampling points were obtained by interpolation with the values at adjacent computational grids.

The mixing index at an axial location was defined to evaluate the degree of mixing of the fluids on a plane perpendicular to the flow direction as follows:

$$IM = \sqrt{\frac{\sigma^2}{\sigma^2_{max}}}, \qquad [2]$$

where $\sigma^2 max$ is the maximum variance over the data range.

The variance was maximal for complete segregation (IM = 0) and minimal for completely mixed fluids (IM = 1). In particular, IM_{out} indicates the IM at the mixer outlet.

Moreover, the intensity of the secondary flows was computed, as an indicator of convective mixing. In particular, the composition of the velocities on a cross-sectional plane was considered, calculated as:

$$\upsilon_{yz} - \sqrt{\upsilon_y^2 + \upsilon_z^2} \qquad [3]$$

where, v_y and v_z are the velocities in the y and z direction, respectively.

Finally, the pressure drop along the channel was also evaluated as another important parameter to be considered when assessing micromixers performance.

RESULTS AND DISCUSSION

The first computational analyses were carried out to investigate the influence of the phase shift *ps*. Simulations indicated that the mixer with no shift in obstacle phase presented the worst behavior, whereas the one with the best performances (both in terms of mixing efficacy and pressure drop) was the 180° phase shifted obstacle, reported as an example in Figure 2 for the geometry C with a fixed cross-section aspect ratio (h/w = 1/3). Concerning

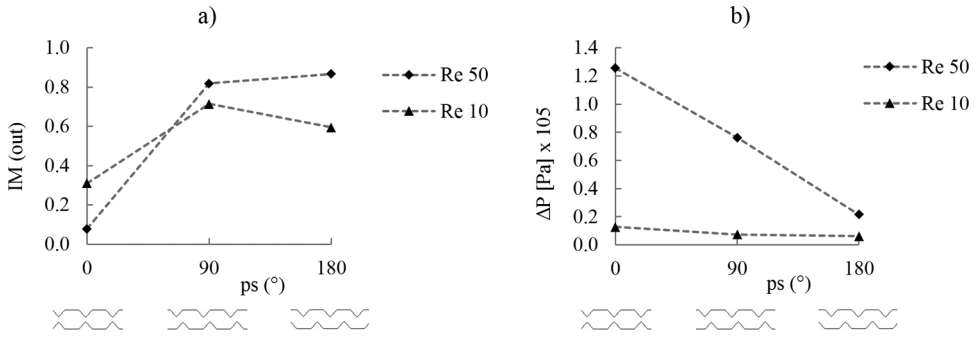

Fig. 2 - *Comparison of geometry C (h/w = 1/3, oh = 0.4) for different obstacle phase shifts at different Reynolds numbers (Re = 10, Re = 50):* ***a)*** *mixing performances and* ***b)*** *pressure losses.*

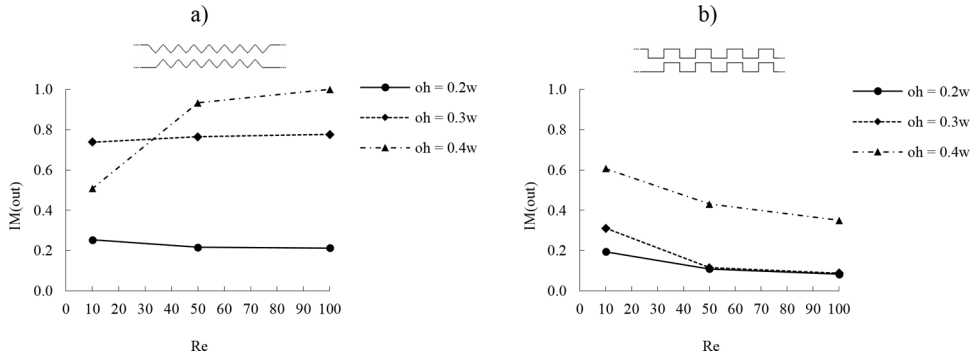

Fig. 3 - *Index of mixing at the channel outlet for the geometries A* ***(a)*** *and E* ***(b)*** *with ps = 180° and h/w = 1/3 for the 3 Reynolds numbers (Re) simulated for different dimension of the obstacles.*

the mixing capability, the geometries with *ps* of 90° and 180° led to an IM_{out} higher than 0.6, whereas the IM_{out} obtained for a *ps* equal 0° were lower than 0.3 (Fig. 2a). Analogous results were obtained for the other configurations investigated. Simulations showed that the presence of a phase shift was essential for enhanced mixing, since it could promote recirculation in the cross-section and therefore allowed more rapid mixing. Moreover, if geometries with different phase shifts were considered, it could be seen that the lowest values of pressure drop could be obtained with a phase shift of 180° (Fig. 2b). In fact, 90° and 180° phase shifts created a sort of tortuous channel, enhancing the mixing and moderating the flow dissipations, whereas a 0° phase shift corresponded to a series of successive flow expansions and contractions which results detrimental for both pressure losses and mixing performances. On the basis of the previous results, it was decided to focus on the channel configurations with a phase shift *ps* of 180° for the subsequent analyses.

The results of the simulations indicated that, keeping *ps* fixed at 180°, different wall geometries and obstacle size provided quite different performances of the micromixers. As an example, Figure 3 shows the IM values at the mixer outlet for geometries A and E (*h*/*w* = 1/3) for 3 simulated Reynolds numbers, considering different dimensions of the obstacles (*oh*/*w* in the range 0.2-0.4).

At first sight, a better performance with generally higher IM_{out} was observed for the geometry A. Moreover, only in that configuration did a beneficial effect of increasing Reynolds number occurred, although this effect in significantly perturbing the flow pattern was clearly obtained only for the amplest dimension of the triangular obstacles (40% of the channel width).

The fact that rectangular obstacles for high Reynolds numbers do not improve the mixing efficiency was likely because in this case mixing relies on pure diffusion only, which is afflicted by an increase of the flow rate.

In contrast, due to an effective convective mixing, the 2 fluids were completely mixed (IM equal to 1) in A geometry with *oh* equal to 0.4·*w* and Reynolds number of 100 after a very short length (about 0.7 mm) of the mixing channel, as shown in Figure 4.

According to the findings described, the additional investigations were performed fixing the dimensions of the obstacles to the highest investigated value (*oh* = 0.4·*w*, i.e., *oh* equal to 60 μm and *ow* equal to 100 μm).

In Figure 5, a comparison among all geometries is shown. In particular, configurations with *ps* = 180° were considered at different Reynolds numbers of 10 and 50 and for different channel aspect ratios. What can easily be observed is that geometries A, B and C (triangular-shaped obstacles) showed an improvement in the mixing performances for increasing Reynolds numbers, while the opposite behavior occurred for geometries D and E (rectangular-shaped obstacles). Moreover, for the totality of analyzed cases, triangular-shaped obstacle geometries gave

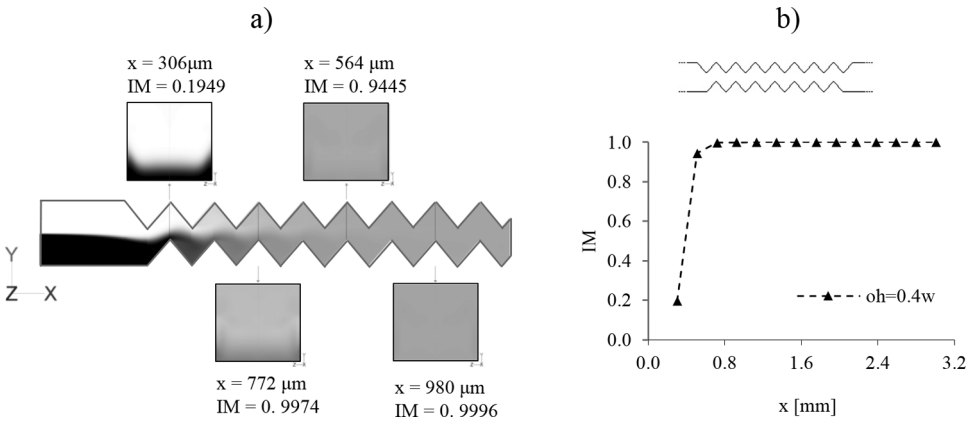

Fig. 4 - *Results for the A geometry for Reynolds number (Re) = 100.* ***a)*** *Concentration map on a plane at half height of the channel and on some cross-sections along the channel with oh = 0.4w;* ***b)*** *Index of mixing throughout the channel.*

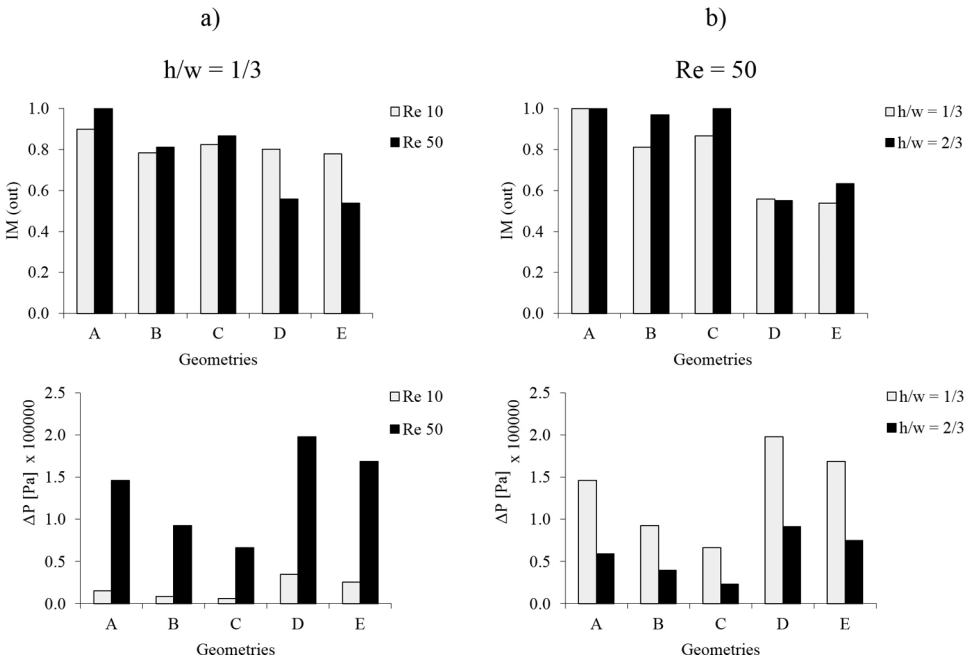

Fig. 5 - *Comparison of the micromixer performances for the 5 wall geometries, with oh/w = 0.4 and ps = 180°. Effect of* ***a)*** *2 different Reynolds numbers (Re) with h/w = 1/3 and* ***b)*** *different heights of the channel with Re = 50, in terms of (top) mixing index (IM) and (bottom) pressure losses. h = height; w = width.*

better performances when compared with the rectangle-shaped obstacle ones. Then, for all of the configurations the influence of the height of the channel was minor, with a general slight improvement of the mixing for the higher cross-section (*h*/*w* equal to 1.5).

Furthermore, the 5 wall geometries were compared in terms of pressure drops caused. As expected, an increase in the pressure losses with the Reynolds number can be observed. As well, pressure drops increased for higher aspect ratio channels. In fact, since the Reynolds number was kept constant, when *h* decreased, the velocity inside the micromixer channel increased. Moreover, geometries A, B and C were less flow resistive than geometries D and E.

In summary, for all of the geometries analyzed, the triangular-shaped obstacle mixers were more effective. Data concerning the rectangular-shaped obstacles suggested that little or no chaotic advection was produced in the square-wave channel for the conditions considered.

On the basis of the previous analyses, 2 mixer geometries with triangular obstacles, *oh*/*w* = 0.4 and *ps* = 180° (i.e., the geometries A and C) were chosen as the best performing (Fig. 6).

As observed in Figure 5a, the mixing performances of these micromixers improved as the Reynolds number increased, due to the generation and enhancement of the secondary flows. Looking at Figure 7, the contribution to the mixing process given by the secondary flows can be appreciated. For low velocities (Re<50), in fact, viscous forces in the fluid dominated inertial forces; therefore, the intensity of secondary flows was poor. For increasing velocities, transverse flow occurred, and a considerable recirculation of the fluids occurred on the whole cross-sectional area of the channel, granting an efficient

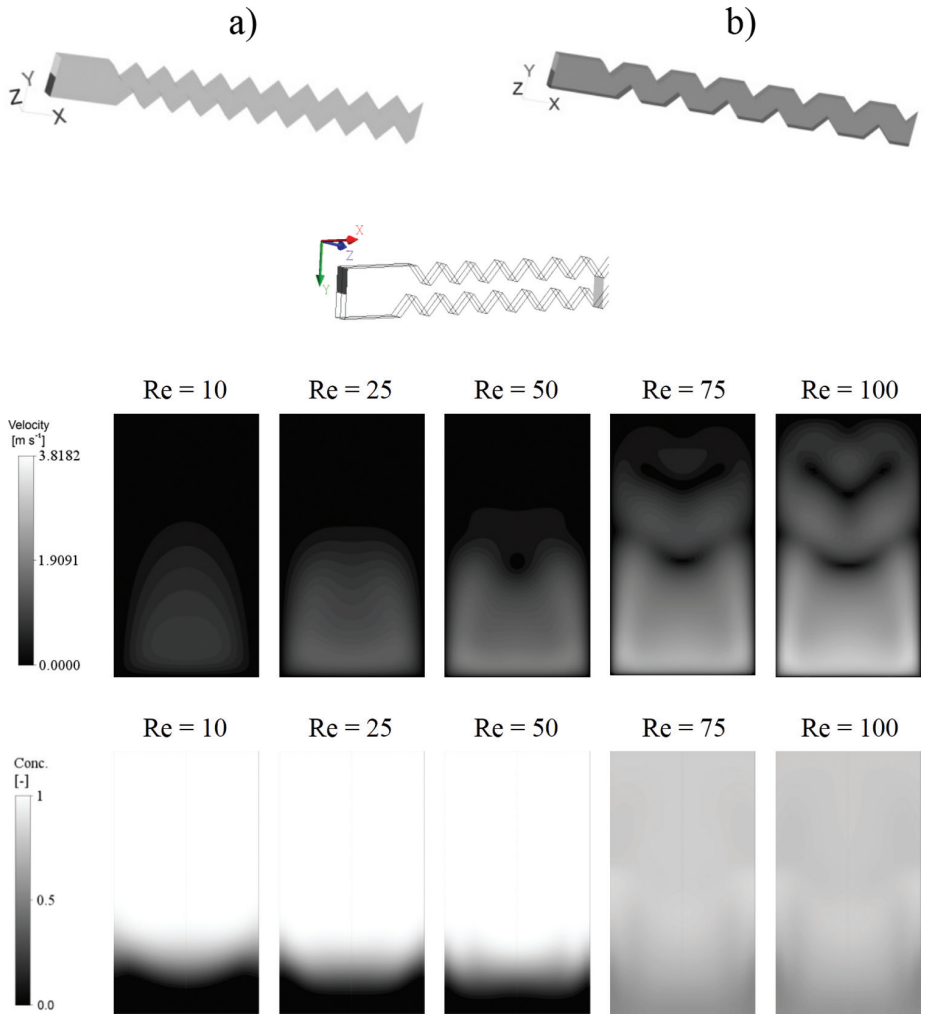

Fig. 6 - *Picture of the 2 geometries considered.* ***a)*** *geometry A;* ***b)*** *geometry C.*

Fig. 7 - ***Top:*** *Intensity of secondary flows v_{yz} for geometry A (ps = 180°, h/w = 1/3) at different velocities;* ***Bottom:*** *concentration maps for geometry A (ps = 180°, h/w = 1/3) at different velocities. Data are referred to a YZ plane placed at x = 0.512 mm from the intersection of the two inlets; h = height; w = width; ps = phase shift.*

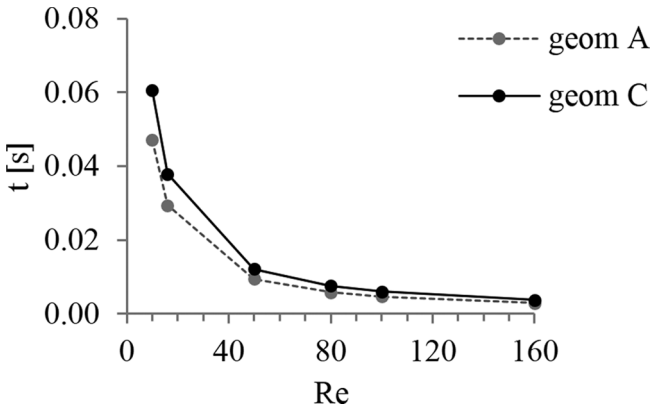

Fig. 8 - *Time needed for the fluids to pass through the microchannel for geometry A and C (ps = 180°, h/w = 2/3) for different Reynolds numbers (Re). ps = phase shift; h = height; w = width.*

mixing. For higher velocities (Re>50), there was a significant increase in the complexity of the flow. This complexity was due to a large increase in the strength of the secondary flows which, in combination with the axial flow, was able to distort and stretch material interfaces and produce chaotic advection. As a result, the interfacial area across which diffusion occurred was greatly increased, which led to rapid mixing. Moreover, although the time needed for the fluid to cross the device was slightly higher for the A geometry, it was lower than 60 milliseconds for both micromixers (Fig. 8). Hence, this quantity was not significant to distinguish the behavior of the 2 devices, because a very short time was required for the mixing process.

In Figure 9 the comparison between the index of mixing for the 2 selected geometries with different heights of the channels is shown for increasing Reynolds numbers. It can be observed that at low Reynolds numbers the most effective mixer was geometry A, while for high Reynolds numbers the 2 micromixers were comparable. This difference in behavior was hardly noticeable for the micromixer with the highest channel aspect ratio (*h/w* = 1/3).

Figure 10a shows the pressure drop trends for geometries A and C, while Figure 10b shows the pressure drops

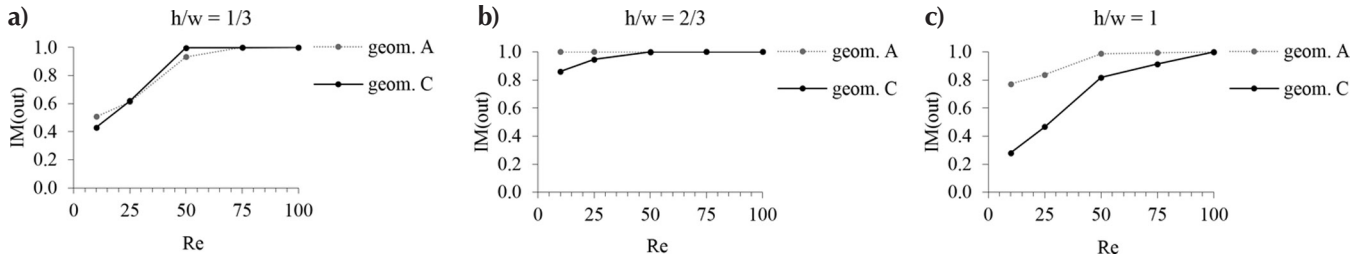

Fig. 9 - *Index of mixing (IM) for geometries A and C (ps = 180°) for different Reynolds numbers (Re) for: h/w = 1/3* ***(a)****, h/w = 2/3* ***(b)****, h/w = 1* ***(c)****. ps = phase shift; h = height; w = width.*

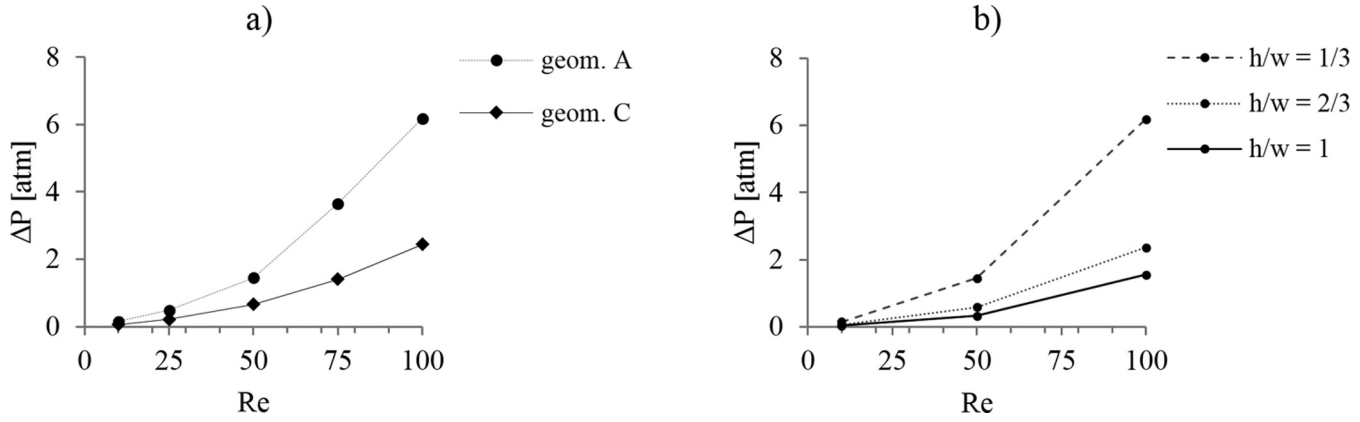

Fig. 10 - *Pressure drops at different Reynolds numbers (Re) for:* ***a)*** *geometries A and C, for h/w = 1/3;* ***b)*** *geometry A for different channel aspect ratios: h/w = 1/3, h/w = 2/3, h/w = 1. h = height; w = width.*

for geometry A for different channel heights. It can be noticed that an increase in the velocity inside the channel led to, as expected, a raise in the pressure drop. The trend was roughly parabolic.

CONCLUSIONS

Fluid flows in microfluidic devices are predominantly laminar, with Reynolds numbers typically ranging from 0.01 to 100 (14). Mixing at very low Reynolds number is dominated by the residence time and depends on the total path of the flow; transverse flows are negligible and thus mixing occurs due to the diffusion of the molecules only, as a result of the residence time and lower overall velocity. In contrast, we investigated mixing improvements in microsystems for $10 < Re < 100$. In this range of Reynolds numbers, both viscous and convective inertial forces are important: at the lowest Reynolds numbers, viscous forces in the fluid dominate convective inertial forces, and fluid velocities in a channel cross-section are essentially 2-dimensional. According to our simulations, mixing enhancement in this regime can be achieved by optimizing the shape of the furrowed channel.

The passive micromixers investigated in the present study have a number of advantages that make them attractive for use in a wide variety of microfluidic applications. First, these channels are easy to fabricate and integrate with other microfluidic components, as the design is relatively simple and can be manufactured using any of the established microfabrication techniques. Moreover, they can be simply integrated on chips because they do not require any form of actuation.

Depending on the Reynolds number, there is also some flexibility in the choice of the channel geometry, as the occurrence of effective chaotic advection occurs for several conformations of the channels presented here. Secondly, for certain applications involving biomolecules, chaotic advection may help minimize damage to large biomolecules, some of which are particularly prone to shear-induced damage. Finally, keeping the flow in a single channel with a height to width ratio near 1 maintains a relatively low surface to volume ratio, which minimizes the chances of clogging or fouling and of any loss of sample by biomolecular adsorption onto the device surface.

In the present work, numerical analyses of mixing in 3-dimensional channels with obstacles on the walls were

performed to investigate mixing behavior and flow characteristics with geometric parameters as well as Reynolds number. Results indicated that furrowed channels with proper triangle-shaped obstacles showed good performance in achieving complete mixing in a very short length of channel and, at the same time, offered low pressure losses.

Financial support: None.

Conflict of interest: The authors have no potential conflict of interest regarding this article.

REFERENCES

1. Nguyen NT, Wu Z. Micromixers: a review. J Micromech Microeng. 2005; 15(2): 1-16.
2. Graveson P, Branjeberg J, Jensen OS. Microfluidics: a review. J Micromech Microeng. 1993; 3(4): 168-182.
3. Nason F, Morganti E, Collini C, et al. Design of microfluidic devices for drug screening on in-vitro cells for osteoporosis therapies. Microelectron Eng. 2011; 88(8): 1801-1806.
4. Sudarsan AP, Ugaz VM. Multivortex micromixing. Proc Natl Acad Sci USA. 2006; 103(19): 7228-7233.
5. Cussler EL. Diffusion mass transfer in fluid systems. 2nd ed. New York: Cambridge University Press; 1996.
6. Kim DS, Lee SH, Kwon TH, Ahn CH. A serpentine laminating micromixer combining splitting/recombination and advection. Lab Chip. 2005; 5(7): 739-747.
7. Schönfeld F, Hessel V, Hofmann C. An optimised split-and-recombine micro-mixer with uniform chaotic mixing. Lab Chip. 2004; 4(1): 65-69.
8. Hessel V, Lowe H, Schonfeld F. Micromixers: a review on passive and active mixing principles. Chem Eng Sci. 2005; 60(8-9): 2479-2501.
9. Hossain H, Ansari MA, Kim KY. Evaluation of the mixing performance of three passive micromixers. Chem Eng J. 2009; 150(2-3): 492-501.
10. Liu RH, Stremler MA, Sharp KV, et al. Passive mixing in a three-dimensional serpentine microchannel. J Microelectromech Syst. 2000; 9(2): 190-197.
11. Aref H. Stirring by chaotic advection. J Fluid Mech. 1984; 143(-1): 1-21.
12. Ansari MA, Kim KY. Parametric study on mixing of two fluids in a three-dimensional serpentine microchannel. Chem Eng J. 2009; 146(3): 439-448.
13. Aubin J, Fletcher DF, Xuereb C. Design of micromixers using CFD modelling. Chem Eng Sci. 2005; 60(8-9): 2503-2516.
14. Anderson RC, Bogdan CJ, Puski A, Su X. Microfluidic biochemical analysis system. Proc Solid-State Sens Actuators. 1997; 1: 477-480.